Disruption of p21 Attenuates Lung Inflammation Induced by Cigarette Smoke, LPS, and fMLP in Mice

Hongwei Yao[1], Se-Ran Yang[1], Indika Edirisinghe[1], Saravanan Rajendrasozhan[1], Samuel Caito[1], David Adenuga[1], Michael A. O'Reilly[2], and Irfan Rahman[1]

Departments of [1]Environmental Medicine and [2]Pediatrics, Lung Biology and Disease Program, University of Rochester Medical Center, Rochester, New York

The cyclin-dependent kinase inhibitor $p21^{CIP1/WAF1/SDI1}$ (p21) is an important inhibitory checkpoint regulator of cell cycle progression in response to oxidative and genotoxic stresses. It is known that p21 potentiates inflammatory response and inhibits apoptosis and proliferation, leading to cellular senescence. However, the role of endogenous p21 in regulation of lung inflammatory and injurious responses by cigarette smoke (CS) or other pro-inflammatory stimuli is not known. We hypothesized that p21 is an important modifier of lung inflammation and injury, and genetic ablation of p21 will confer protection against CS and other pro-inflammatory stimuli (lipopolysacchride [LPS] and N-formyl-methionyl-leucyl-phenylalanine [fMLP])-mediated lung inflammation and injury. To test this hypothesis, p21-deficient (p21−/−) and wild-type mice were exposed to CS, LPS, or fMLP, and the lung oxidative stress and inflammatory responses as well as airspace enlargement were assessed. We found that targeted disruption of p21 attenuated CS-, LPS-, or fMLP-mediated lung inflammatory responses in mice. CS-mediated oxidative stress and fMLP-induced airspace enlargement were also decreased in lungs of p21−/− mice compared with wild-type mice. The mechanism underlying this finding was associated with decreased NF-κB activation, and reactive oxygen species generation by decreased phosphorylation of $p47^{phox}$ and down-modulating the activation of p21-activated kinase. Our data provide insight into the mechanism of pro-inflammatory effect of p21, and the loss of p21 protects against lung oxidative and inflammatory responses, and airspace enlargement in response to multiple pro-inflammatory stimuli. These data may have ramifications in CS-induced senescence in the pathogenesis of chronic obstructive pulmonary disease/emphysema.

Keywords: NF-κB; inflammation; chronic obstructive pulmonary disease; emphysema; senescence

Chronic obstructive pulmonary disease (COPD) is the fourth leading cause of chronic morbidity and mortality in the United States, and is characterized by chronic inflammation and distinct structural alterations of the small airways (airway remodeling) (1–3). Cigarette smoke (CS) is the major risk factor for the development of COPD. It contains an estimated 10^{15} to 10^{17} oxidants/free radicals and approximately 4,700 different chemical compounds, including reactive aldehydes and quinones, per puff (4). We, and others, have shown that CS exposure causes lung inflammation due to the influx of macrophages, neutrophils, dendritic cells, and $CD8^+$ T lymphocytes, leading to increased levels of pro-inflammatory mediators (5–11). However, the cellular and molecular mechanisms underlying CS-mediated abnormal lung inflammation and airspace enlargement in the development of COPD are not well understood. Recently, it has been postulated that cellular senescence and proliferation/apoptosis are involved in the pathophysiology of emphysema/COPD (12–14).

CLINICAL RELEVANCE

Inhibition of p21 will protect lungs against cigarette smoke (CS)–mediated oxidative and inflammatory responses, as well as airspace enlargement. Activation of p21 gene will have ramifications in CS-induced senescence and apoptosis in the pathogenesis of chronic obstructive pulmonary disease/emphysema.

Cell division is a highly regulated process, with checkpoints to ensure that DNA is faithfully copied and that identical chromosomal copies are distributed equally to each daughter cell (15). These checkpoints also respond to damage, enabling the cell cycle to be arrested to provide time for transcription and activation of genes that facilitate repair. Passage through the restriction point and entry into S phase is controlled by cyclin/cyclin-dependent kinase (CDK) complexes (16, 17). Active cyclin/CDK complexes phosphorylate and inactivate members of the retinoblastoma protein family that are negative regulators of G_1 and S-phase progression, leading to induction of E2F-regulated gene expression and cell proliferation. CDK inhibitors bind and inhibit the activity of cyclin/CDK complexes and negatively regulate cell cycle progression (16, 18). These proteins play important roles in regulating proliferation during normal development and differentiation and after genotoxic stress. $p21^{CIP1/WAF1/SDI1}$ (p21) is a member of a family of cell cycle inhibitors that includes p27 and p57 (19), and is capable of inhibiting a broad range of cyclin/CDK complexes and hence cell proliferation so as to allow cells to repair the DNA damage (20).

It has also been shown that p21 potentiates inflammatory response and inhibits apoptosis and proliferation, leading to cellular senescence (21, 22). This is supported by the observations that p21-deficient (p21−/−) mice are resistant to serum transfer–induced inflammatory arthritis (23), and peritoneal macrophages from p21−/− mice exhibit a higher phagocytotic capacity and lower expression of cytokines such as IL-1β, macrophage inflammatory protein (MIP)-1, and MIP-2 than do their wild-type (WT) counterparts (24). Moreover, genetic knockout of p21 attenuated angiotensin II–induced NF-κB activation by decreasing the production of reactive oxygen species (ROS) *in vitro* and *in vivo* (25). Similarly, p21 has been shown to stimulate NF-κB activity through its effect on the CBP/p300 transcription cofactor family (26), and targeted disruption of p21 was associated with decreased NF-κB activation in glial cells in response to lipopolysaccharide (LPS) (27). All of these findings highlighted an important role of p21 in modifying inflammatory response and ROS production. Most importantly, recent studies showed that p21 expression was increased in

(*Received in original form September 20, 2007 and in final form January 3, 2008*)

This study was supported by National Institutes of Health R01-HL085613 to I.R., NIEHS-ES01247, and NIEHS Toxicology Training grant ES07026.

Correspondence and requests for reprints should be addressed to Irfan Rahman, PhD, Department of Environmental Medicine, Lung Biology and Disease Program, University of Rochester Medical Center, 601 Elmwood Ave., Box 850, Rochester, NY 14642. E-mail: irfan_rahman@urmc.rochester.edu

Am J Respir Cell Mol Biol Vol 39. pp 7–18, 2008
Originally Published in Press as DOI: 10.1165/rcmb.2007-0342OC on January 31, 2008
Internet address: www.atsjournals.org

alveolar macrophages from smokers (28), and in lung epithelial cells as well as in fibroblasts in response to CS (29–31). In addition, oxidant-induced DNA damage prolonged the expression of p21 (32). Thus, it is possible that oxidative stress induced by CS may contribute to the prolonged induction of p21 (cell cycle arrest), which leads to propagation of lung inflammatory response by activation of NF-κB. However, the role of endogenous p21 in regulation of lung oxidative, inflammatory, and injurious (emphysematous) responses by CS exposure or by any inflammatory agents is not known.

It has been shown that 5 to 6 months of CS exposure is usually required to induce emphysema in C57BL/6J mice. Therefore, we used an N-formyl-methionyl-leucyl-phenylalanine (fMLP)-induced airspace enlargement model, which induces emphysema in only 21 days and mimics chronic CS-induced emphysema (33–35), and investigated the role of p21 in airspace enlargement. We hypothesized that targeted disruption of p21 protects lungs against detrimental effect of CS and other pro-inflammatory agents, such as LPS and fMLP. To test this hypothesis, p21-deficient (p21−/−, defective in G1 checkpoint control) and WT mice were exposed to CS, LPS, or fMLP, and the lung oxidative and inflammatory responses as well as airspace enlargement/emphysema were assessed.

MATERIALS AND METHODS

Mice

Male C57BL/6J WT mice (7–9 wk old) were purchased from the Jackson Laboratory (Bar Harbor, ME), and p21−/− mice (36) were obtained from Dr. Philip Leder at Harvard Medical School (Boston, MA), and backcrossed 10 generations onto C57BL/6J strain and housed in the Vivarium Facility of the University of Rochester before being exposed to CS, LPS, or fMLP. All p21−/− mice used in the present study were homozygous. All animal procedures were approved by the University Committee on Animal Research of the University of Rochester.

CS Exposure

Eight- to ten-week-old mice (6–8 mice per group) were used for CS exposure. In brief, mice were housed in an individual wire cage compartment, which was placed inside an aerated plastic box connected to the smoke source. Research-grade cigarettes (2R4F [total particulate matter {TPM} concentration 11.7 mg/cigarette, tar 9.7 mg/cigarette, nicotine 0.85 mg/cigarette]; University of Kentucky, Lexington, KY) were used to generate smoke, and mice were exposed to CS according to the Federal Trade Commission protocol (1 puff/min of 2-s duration and 35-ml volume) using a Baumgartner-Jaeger CSM2072i automatic CS-generating machine (CH Technologies, Westwood, NJ). Mainstream CS was diluted with filtered air and directed into the exposure chamber. The smoke exposure (TPM in per cubic meter of air) was monitored in real time with a MicroDust Pro-aerosol monitor (Casella CEL, Bedford, UK) and verified daily by gravimetric sampling (5, 6, 37, 38). The smoke concentration was set at a nominal value of approximately 300 mg/m^3 TPM by adjusting the flow rate of the diluted medical air (5, 37–40), and the level of carbon monoxide in the chamber was 350 ppm. The level of carboxyhemoglobin (COHb) in blood was 15%, which was consistent with previous studies (39, 41). Mice received two 1-hour exposures, 1 hour apart, for 3 consecutive days, and killed 24 hours after the last exposure. Control mice were exposed to filtered air in an identical chamber according to the same protocol described for CS exposure.

LPS Aerosolization

Age-matched C57BL/6L WT and p21-deficient mice were exposed to an aerosol of saline alone or saline containing *Escherichia coli* LPS (1 mg/ml; Sigma, St. Louis, MO) for 8 minutes as described previously (5). Twenty-four hours after LPS aerosolization, mice were anesthetized and killed.

fMLP Aerosolization

Age-matched WT and p21−/− mice were exposed to aerosolized saline alone or saline containing fMLP (5 mg/ml; Sigma) for 8 minutes as described previously (33–35). At Day 3, the same dose of fMLP was exposed again to make sure that all the mice received fMLP. Twenty-one days after the first aerosolization, animals from all groups were anesthetized and killed. This dose and duration of fMLP are known to induce increased airspace enlargement in mice (33–35).

Bronchoalveolar Lavage

Mice were injected with 100 mg/kg (body weight) of pentobarbiturate (Abbott laboratories, Abbott Park, IL) intraperitoneally and killed by exsanguination. The heart and lungs were removed *en bloc*, and the lungs were lavaged three times with 0.5 ml of 0.9% sodium chloride. The lavage fluid was centrifuged, and the cell-free supernatants were frozen at −80°C for later analysis. The bronchoalveolar lavage (BAL) cell pellet was resuspended in 1 ml of 0.9% sodium chloride, and the total cell number was determined by counting on a hemocytometer. Differential cell counts (minimum of 400 cells per slide) were performed on cytospin-prepared slides (Thermo Shandon, Pittsburgh, PA) stained with Diff-Quik (Dade Behring, Newark, DE).

Histologic Analysis

Mouse lungs (which had not been lavaged) were inflated with 1% low melt agarose at a pressure of 25 cm H_2O and then fixed with 4% neutral buffered paraformaldehyde. Tissues were embedded in paraffin, sectioned (4 μm), and stained with hematoxylin and eosin (H&E). Alveolar size was estimated from the mean linear intercept (Lm) of the airspace as described (42–45). In brief, mid-saggital sections were obtained from the left lung and stained with H&E. Digital photomicrographs were taken across the widest transect of each section and a grid was superimposed. Mean linear intercept was calculated using the formula $Lm = 2L_T/I_W$, where L_T is the total length of the grid in microns, and I_w is the number of times the grid intersects an alveolar wall for each sample based on 10 random fields observed at a magnification of ×200 using a cross-line.

For macrophage immunohistochemistry, lung sections were deparaffinized and hydrated by passing through a series of xylene and graded alcohol. Endogenous peroxidase activity was quenched by exposure to 3% H_2O_2 in methanol for 30 minutes. Nonspecific binding of antibodies to the tissues was blocked by incubating the tissue with 5% normal goat serum in 0.5% BSA in PBS for 30 minutes. For the detection of macrophages, rat anti-mouse Mac-3 monoclonal antibody (BD Pharmingen, San Diego, CA) at a titer of 1:50 was used. A biotinylated goat anti-mouse/rabbit Ig (DAKO Corp., Santa Barbara, CA) was used at a titer of 1:100. Tissues were incubated with primary antibodies overnight at 4°C. After being washed, tissues were incubated with secondary antibody for 30 minutes. 3,3′-diaminobenzidine (DAKO Corp.) was used as peroxidase substrate. In each instance, sections from different time points were processed together with equal time for color development. Tissues were counterstained with hematoxylin. The number of Mac-3–positive cells in the lung sections (5 random microscopic fields per lung section in three different sections) were counted manually in blinded manner under ×200 magnification and averaged (39, 45, 46).

Myeloperoxidase Assay

Myeloperoxidase (MPO) activity was determined in lung homogenates as described previously (5, 47), with slight modification. In brief, the lung tissues were homogenized in 10 vols of 100 mM phosphate buffer (pH 7.4) containing protease inhibitors. To determine the MPO activity in enzymatic extract, we used a spectrophotometric method with tetramethylbenzidine (TMB; Sigma). Briefly, the assay mixture consisted of 400 μl of phosphate buffer (100 mM, pH 5.4) with 0.5% hexadecyltrimethylammonium bromide (Sigma-Aldrich, MO), 40 μl TMB (20 mM in dimethyl sulfoxide, prepared fresh and protected from light) and H_2O (23 μl). To this assay mixture, 20 μl of enzyme extract was added, the mixture was incubated at 37°C for 3 minutes, and finally 17 μl of H_2O_2 (0.03%) was added. The mixture was further incubated for 3 minutes. The reaction was stopped by adding 2 ml of acetate

buffer (0.2 M, pH 3.2). The tubes were kept on ice and the absorbance was read at 655 nm. The appropriate reagent blank was prepared by using a buffer instead of the tissue extract. The activity was expressed in the samples as Units/mg protein.

Lipid Peroxidation Products Assay in Lung Homogenate

Lung tissues were homogenized with ice-cold 20 mM Tris-HCl (pH 7.4) and diluted to approximately 10% (wt/vol). The homogenates were centrifuged at 3,000 rpm for 10 minutes at 4°C and the supernatants were collected. Butylated hydroxytoluene (5 mM; Sigma) was added to the supernatant to prevent further peroxidation and the samples were immediately frozen in liquid nitrogen. Lipid peroxidation products (malondialdehyde [MDA] and 4-hydroxy-2-nonenal [4-HNE]) were measured using a lipid peroxidation kit (Calbiochem, San Diego, CA). For MDA and 4-HNE assays, 200 μl of supernatant was added to 650 μl of 10.3 mM N-methyl-2-phenylindole in acetonitrile, vortexed, 150 μl of 15.4 mM methanesulfonic acid was added, and the whole was incubated at 45°C for 40 minutes. The samples were cooled on ice and absorbance was measured at 586 nm using a microplate reader (Bio-Rad, San Diego, CA).

Measurement of Superoxide Anion Release in BAL Cells

ROS release of BAL cells was quantified using a spectrophotometric method based on the superoxide dismutase (SOD)-inhibitable reduction of ferricytochrome *c* as described by Johnston (48). Each tube contained 10^5 cells, and 80 μmol of ferricytochrome *c* from equine heart (Sigma) in phosphate-buffered saline (PBS). Superoxide anion release was measured under two conditions, spontaneously and after phorbol myristate acetate (PMA) stimulation for 80 minutes at 37°C. PMA was freshly prepared by diluting a stock solution in PBS to a final concentration of 1.6 μM. Paired tubes were established with and without SOD from bovine erythrocytes (240 $IU \cdot ml^{-1}$ final concentration; Sigma) to assess the specificity of cytochrome *c* reduction as control. Optical density was then determined with absorbance at 550 nm. The resulting change in absorbance between the experimental group and its control (same sample supplemented with SOD) was used to calculate the nanomoles of superoxide anion produced by application of the molar extinction coefficient ($\sum 550$) of cytochrome *c* ($21 \times 10^3\ M^{-1} \cdot cm^{-1}$) in the following formula: $\Delta absorbance / \sum 550 \times$ light path = concentration.

ROS Determination by 2′,7′-Dichlorofluorescein-Diacetate Staining in BAL Cells

ROS release was determined using 2′,7′-dichlorofluorescein-diacetate (DCF-DA), which is an oxidant-sensitive fluorescent probe. Inside the cell, the probe is deacetylated by esterases and formed H_2DCF which is oxidized by ROS to DCF, a highly fluorescent compound (49). ROS generation in BAL cells was assessed using the probe DCF-DA. Briefly, the cytospin slides were incubated with 10 μM DCF-DA (Molecular Probes, Eugene, OR) for 15 minutes at room temperature. After being rinsed with PBS, the slides were observed under the fluorescent microscope and assessed with a score between 1 and 3 based on the following criteria: 1, weak staining; 2, moderate staining; 3, intense staining.

Extraction of Cytoplasmic and Nuclear Proteins from Lung Tissue Samples

One hundred milligram of lung tissue was mechanically homogenized in 0.5 ml of ice-cold buffer A (10 mM HEPES [pH 7.8], 10 mM KCl, 2 mM $MgCl_2$, 1 mM DTT, 0.1 M EDTA, 0.2 mM NaF, 0.2 mM Na orthovandate, 1% [vol/vol] NP-40, 0.4 mM phenylmethylsulfonyl fluoride, and 1 μg/ml leupeptin). The homogenate was centrifuged at 2,000 rpm in a benchtop centrifuge for 30 seconds at 4°C to remove cellular debris. The supernatant was then transferred to a 1.7 ml ice-cold Eppendorf tube and further centrifuged for 30 seconds at 13,000 rpm at 4°C. The supernatant was collected as a cytoplasmic extract. The pellet was resuspended in 200 μl of buffer C (50 mM HEPES [pH 7.8], 50 mM KCl, 300 mM NaCl, 0.1 M EDTA, 1 mM DTT, 10% [vol/vol] glycerol, 0.2 mM NaF, 0.2 mM Na orthovandate, and 0.6 mM phenylmethylsulfonyl fluoride) and placed on the roller in the cold room for 30 minutes. After centrifugation at 13,000 rpm in an Eppendorf tube for 5 minutes, the supernatant was collected as the nuclear extract, and stored at −80°C until use.

Assay of Pro-Inflammatory Mediators

The levels of pro-inflammatory mediators (keratinocyte chemoattractant [KC], IL-6, monocyte chemotactic protein [MCP]-1, IL-1β, and TNF-α) in lung homogenates were measured by the Luminex 100 using the beadlyte mouse multi-cytokine beadmaster kit (Upstate, NY) according to the manufacturer's instructions. The assays permit simultaneous cytometric quantitation of multiple chemokines/cytokines with minimal sample volume. The assays use microspheres as the solid support for immunoassays. The results were expressed in the samples as pg/mg protein.

In peritoneal macrophages, the culture medium was collected after treatment and centrifuged at 2,500 rpm for 5 minutes to pellet the cells. The levels of MCP-1 and KC in the supernatant were determined by enzyme-linked immunosorbent assay from respective duo-antibody kits (R&D Systems, Minneapolis, MN) according to the manufacturer's instructions.

Protein Assay

Protein level was measured with a BCA kit (Pierce, Rockford, IL). Protein standards were obtained by diluting a stock solution of BSA. Linear regression was used to determine the actual protein concentration of the samples.

Western Blot Analysis

Lung tissue homogenate samples, including cytoplasmic and nuclear proteins, were separated on a 7.5 to 12% SDS-PAGE. Separated proteins were electroblotted onto nitrocellulose membranes (Amersham, Arlington Heights, IL), and blocked for 1 hour at room temperature with 5% nonfat dry milk. The membranes were then probed with 1:400 to 1:1,000 diluted antibodies of anti-phospho-NF-κB p65 (ser276 or ser536) (Cell Signaling Technology, Beverly, MA) and anti-RelA/p65 (Santa Cruz Biotechnology, Santa Cruz, CA) to determine respective proteins and anti-γp21-activated kinase (γPAK; Santa Cruz Biotechnology) and anti-pS^{141}-PAK (Biosource International, Inc., Carlsbad, CA) to detect respective cytoplasmic protein. After three washing steps (10 min each), the levels of protein were detected using second antibody (1:5,000 dilution in 2.5% nonfat dry milk in PBS containing 0.1% Tween 20 [vol/vol] for 1 h) linked to horseradish peroxidase (Dako, Santa Barbara, CA), and bound complexes were detected using enhanced chemiluminescence method (PerkinElmer, Waltham, MA). Equal loading of the sample was determined by quantitation of protein as well as by reprobing membranes for β-actin.

IKKβ Activity Assay in Lung Tissue

Lung tissue was homogenized in lysis buffer (50 mM HEPES, 150 mM NaCl, 1 mM EDTA, 1.5 mM $MgCl_2$, 10% glycerol, 1% Triton X-100, 1 mM Na_3VO_4, 10 mM NaF, 1 μg of leupeptin/ml, 1 μg of aprotinin/ml, and 400 μM PMSF). After incubation on ice for 20 minutes, cell debris was removed by centrifugation at 4°C (13,000 rpm, 15 min). The protein concentration was determined as described above, and samples were kept frozen in aliquots at −70°C. The lung homogenates were then immunoprecipitated with 2 μg of anti-IKKβ antibody (Santa Cruz Biotechnology) in the presence of 20 μl of Sepharose-protein A beads (Sigma) overnight at 4°C. The beads were washed three times with lysis buffer and two times with kinase assay buffer (20 mM HEPES, 20 mM $MgCl_2$, and 2 mM DTT). The kinase reaction was performed in 40 μl ATP-master buffer (20 μM of ATP, 10 μCi of [^{32}P]ATP and 4.0 μg of GST-IκBα in kinase buffer). The reaction was incubated at 30°C for 30 minutes and was terminated by addition of 10 μl of 5× SDS-PAGE sample buffer. Incorporation of ^{32}P into the substrate was visualized by autoradiography after electrophoresis. Western blotting for IKKβ was performed as a loading control by using anti-IKKβ antibody.

Preparation of CS Extract

Research-grade cigarettes (1R3F) were obtained from the Kentucky Tobacco Research and Development Center at the University of Kentucky. The composition of 1R3F/cigarettes was: TPM, 17.1 mg;

tar, 15 mg; and nicotine, 1.16 mg. CS extract (CSE, 10%) was prepared by bubbling smoke from one cigarette into 10 ml of culture media at a rate of one cigarette/2 minutes as described previously (6, 10), using a modification of the method described earlier by Carp and Janoff (50). The pH of the CSE was adjusted to 7.4, and was sterile filtered through a 0.45-μm filter (25 mm Acrodisc; Pall Corporation, Ann Arbor, MI). CSE preparation was standardized by measuring the absorbance (OD 0.74 ± 0.05) at a wavelength of 320 nm. The pattern of absorbance (spectrogram) observed at λ_{320} showed a very little variation between different preparations of CSE. CSE was freshly prepared for each experiment and diluted with culture media supplemented with 1% fetal bovine serum (FBS) immediately before use. Control medium was prepared by bubbling air through 20 ml of serum-free RPMI, adjusting pH to 7.4, and sterile filtering as described above.

Elicitation and Culture of Peritoneal Macrophages

The mice were subjected to peritoneal lavage with PBS 4 days after injection with 2 ml of 4% autoclaved aged thioglycollate broth (Sigma). The peritoneal macrophages were washed with PBS and were grown in 6-well plates with RPMI 1640 medium (Life Technologies, Gaithersburg, MD) supplemented with 10% FBS (HyClone Laboratories, Logan, UT), 2 mM L-glutamine, 100 μg/ml penicillin, 100 U/ml streptomycin, 1% nonessential amino acids, 1% sodium pyruvate, 1 μg/ml human holotransferrin, and 1 mM oxaloacetic acid at 37°C in a humidified atmosphere containing 5% CO_2. After 2 hours of incubation, wells were gently pipetted to remove nonadherent cells, and adherent cells were continuously cultured overnight before treatment.

Treatment of Peritoneal Macrophages

After starvation for 6 hours with RPMI 1640 medium containing 1% FBS before treatment, the cells were treated with CSE (0.1, 0.2, 0.4%) for 24 hours at 37°C with 5% CO_2. All treatments were performed in duplicate. Culture media from these peritoneal macrophages were collected and stored at −80°C for KC and MCP-1 assay.

Statistical Analysis

The results are shown as the mean ± SEM. Statistical analysis of significance was calculated using one-way Analysis of Variance (ANOVA) followed by Tukey's *post hoc* test for multigroup comparisons using STATVIEW.

RESULTS

Inflammatory Cell Influx into the Lung and Airspace Enlargement Was Decreased in p21−/− Mice in Response to CS Exposure, LPS, or fMLP Aerosolization

To determine the role of p21 in CS-mediated lung inflammatory response, WT C57BL/6J and p21−/− mice were exposed to CS, and neutrophil influx into BAL fluid and lung tissue was assessed by Diff-Quick and H&E staining, respectively. CS exposure resulted in significant influx of neutrophils in BAL fluid of WT mice, which was attenuated in p21−/− mice (Figure 1A). The total number of macrophages in BAL fluid was not altered in response to acute CS exposure in WT and p21−/− mice (Figure 1D). Similarly, neutrophils influx into BAL fluid was significantly decreased in p21−/− mice compared with WT mice, whereas the total number of macrophages in BAL fluid remained unchanged in WT and p21−/− mice in response to LPS and fMLP aerosolization (Figures 1B, 1C, 1E, and 1F). Genetic ablation of p21 significantly decreased the inflammatory cells influx into the lungs in response to CS exposure or LPS aerosolization, as shown by H&E staining (Figures 2A and 2B). Twenty-one days after the first fMLP aerosolization, the lungs from WT mice showed enlargement of airspace with destruction of alveolar septa as reflected by increased *Lm* in WT mice (Figure 2C). However, no injurious response was observed in lungs of p21−/− mice in response to fMLP aerosolization (Figure 2C). Macrophage infiltration, which was stained with Mac-3 immunohistochemistry, was also significantly reduced in the lungs of p21−/− mice as compared with WT mice in response to CS exposure (Figure 3). These results suggested that targeted disruption of p21 attenuated lung inflammatory cell influx and airspace enlargement in response to CS exposure, LPS, or fMLP aerosolization.

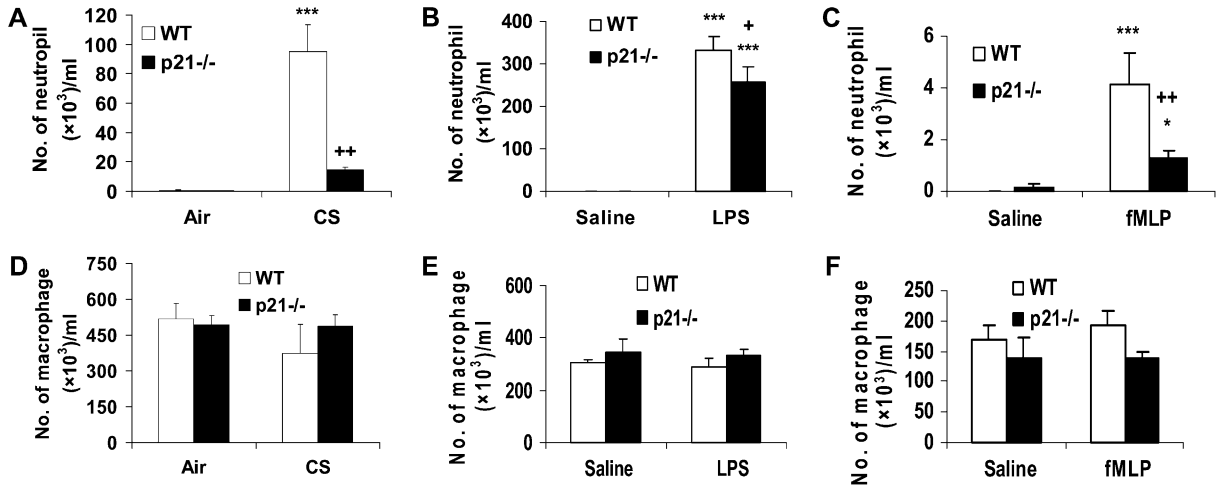

Figure 1. The number of neutrophils, but not macrophages, was decreased in bronchoalveolar lavage (BAL) fluid of p21−/− mice in response to cigarette smoke (CS) exposure, lipopolysaccharide (LPS), or N-formyl-methionyl-leucyl-phenylalanine (fMLP) aerosolization. Mice were exposed to CS, LPS, or fMLP as described in MATERIALS AND METHODS. After killing, the lungs were lavaged and cytospin slides were prepared. Total cells in BAL fluid were counted using a hemocytometer. At least 400 cells were counted in a blinded manner to determine the differential cell count using cytospin slides stained with Diff-Quick. The number of neutrophils in BAL fluid was decreased in p21−/− mice in response to (*A*) CS exposure, (*B*) LPS, or (*C*) fMLP aerosolization compared with respective wild-type (WT) mice. However, the number of macrophages in BAL fluid was not altered in p21−/− mice compared with WT mice in response to (*D*) CS exposure, (*E*) LPS, or (*F*) fMLP aerosolization. Data are shown as mean ± SEM (n = 4–5 per group). *$P < 0.05$, ***$P < 0.001$, significant compared with respective air- or saline-exposed groups; $^{+}P < 0.05$, $^{++}P < 0.01$, significant compared with CS-, LPS-, or fMLP-exposed WT mice.

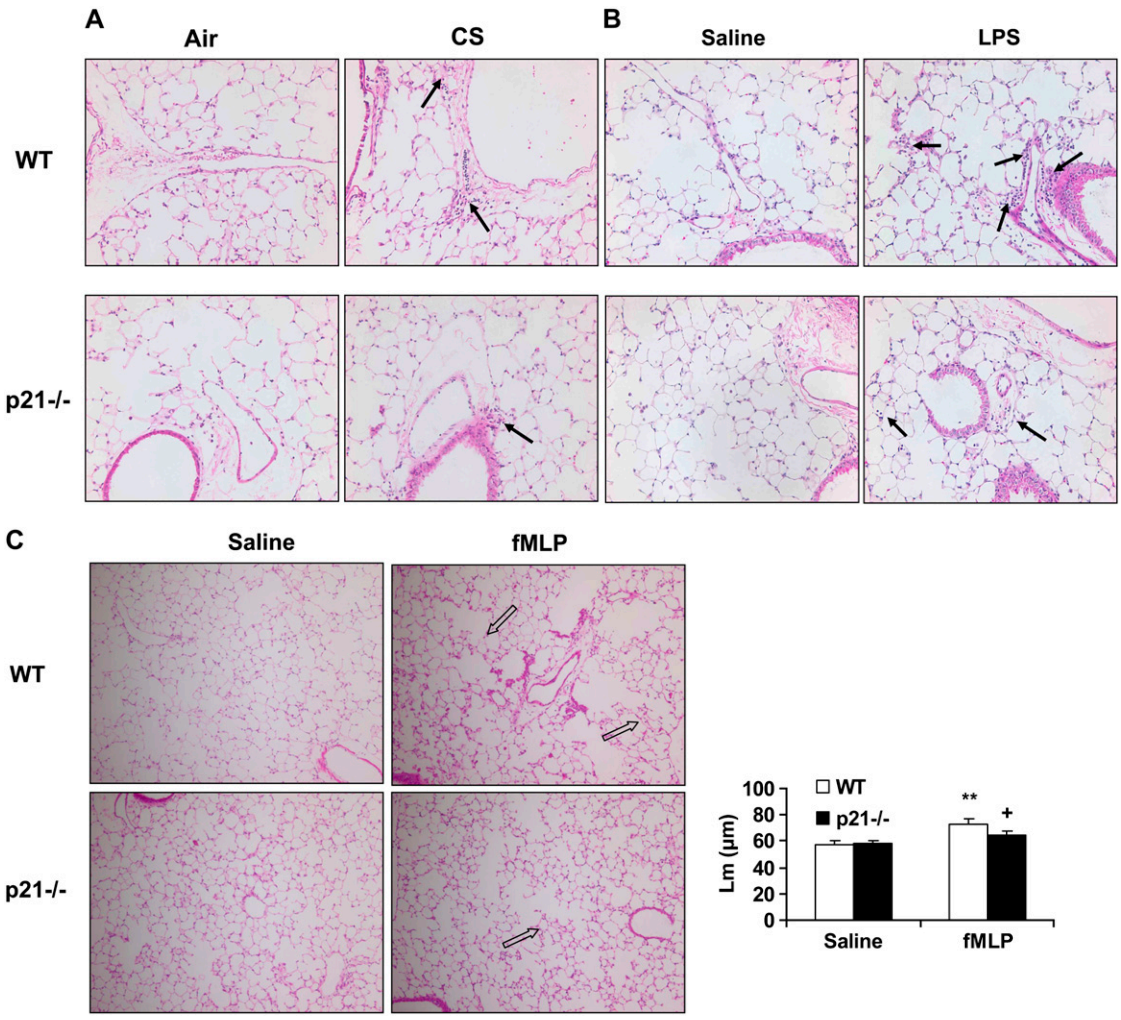

Figure 2. Reduced inflammatory cell influx or injurious response in lungs of p21−/− mice exposed to CS, LPS, or fMLP aerosolization. Mice were exposed to CS, LPS, or fMLP as described in MATERIALS AND METHODS. After sacrificing, the left lung was fixed, embedded in paraffin, and stained with hematoxylin and eosin (H&E). Genetic ablation of p21 decreased inflammatory cell influx into the lungs in response to (*A*) CS exposure or (*B*) LPS aerosolization. In addition, fMLP-induced enlargement of airspace and destruction of alveolar septa were attenuated in p21−/− mice as compared with WT mice (*C*). The H&E-stained pictures represent three separate experiments. *Solid arrows* indicate inflammatory cells, and *open arrows* indicate enlargement of airspace with destruction of alveolar septa. *Original magnification*: *A* and *B*, ×200; *C*, ×100. $^{**}P < 0.01$, significant compared with respective saline-exposed groups; $^{+}P < 0.05$, significant compared with fMLP-exposed WT mice.

MPO Activity and Phosphorylation of p21-Activated Kinase on ser141 Residue Were Decreased in Lungs of p21−/− Mice in Response to CS Exposure or LPS Aerosolization

The activity of MPO is used to estimate the level of neutrophilic inflammation in the tissue (5, 47). We assessed the activity of MPO in lungs of WT and p21−/− mice to further determine the pro-inflammatory role of p21 in response to CS exposure. CS exposure led to an increase in MPO activity in the lungs of WT mice that was reduced in p21−/− mice (Figure 4A). Similarly, genetic ablation of p21 significantly decreased lung MPO activity

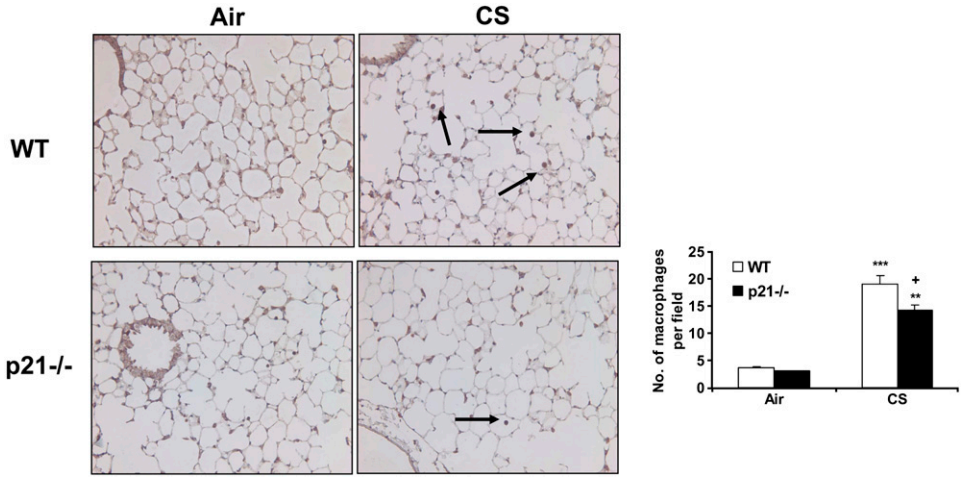

Figure 3. Macrophage influx into the lungs was reduced in p21−/− mice exposed to CS. Macrophages were detected with immunohistochemical staining using anti-mouse Mac-3 antibody in lung sections from CS-exposed mice. The number of macrophages in the lungs was decreased in p21−/− mice compared with WT mice exposed to CS. The pictures represent at least three staining experiments (n = 4–5 per group). *Arrows* indicate macrophages. *Original magnification*: ×200. $^{**}P < 0.01$, $^{***}P < 0.001$, significant compared with respective air-exposed groups; $^{+}P < 0.05$, significant compared with CS-exposed WT mice.

in response to LPS aerosolization (Figure 4B). PAK activation due to its phosphorylation are known to cause neutrophil migration into lung interstitial and alveolar space in response to LPS inhalation (51). The level of phosphorylated PAK on ser141 residue was significantly reduced in the lungs of p21−/− mice compared with WT mice in response to CS exposure (Figures 5A and 5B), corroborating with decreased neutrophil infiltration into the lungs of p21−/− mice exposed to CS.

Levels of Pro-Inflammatory Mediators Were Decreased in Lungs of p21−/− Mice in Response to CS exposure, LPS, or fMLP Aerosolization

CS is a strong inflammatory stimulus that induces the release of pro-inflammatory mediators such as IL-6, KC, and MCP-1, and recruits macrophages and neutrophils into the lung tissue (6, 37, 38). Therefore, we investigated whether p21−/− mice exhibited an altered level of representative cytokines/chemokines in the lungs in response to CS exposure. Our data showed that CS exposure increased the levels of KC, MCP-1, IL-6, and TNF-α in the lungs and that these levels were significantly decreased in p21−/− mice (Figure 6A). The levels of KC, MCP-1, IL-6 and IL-1β were also significantly reduced in the lungs of p21−/− mice compared with WT mice exposed to aerosolized LPS (Figure 6B). Furthermore, targeted disruption of p21 reduced the release of KC and MCP-1 in lungs in response to fMLP aerosolization (Figure 6C). These results further demonstrated the attenuation of inflammatory response induced by CS exposure, LPS, and fMLP aerosolization in the lung of p21−/− mice.

ROS Release in BAL Cells and Levels of Lipid Peroxidation Products Were Decreased in Lung Tissue of p21−/− Mice Exposed to CS

It has been shown that macrophages and neutrophils obtained from peripheral blood or lungs of smokers release increased levels of ROS (52). To demonstrate the regulatory effect of p21 on ROS release, the levels of ROS in BAL cells were assessed with a method based on SOD-inhibitable reduction of ferricytochrome *c* in WT and p21−/− mice exposed to CS. CS exposure led to increased release of ROS in BAL cells, but the levels were decreased in p21−/− mice compared with WT mice exposed to CS (Figure 7A). Similarly, DCF-DA staining showing that targeted disruption of p21 attenuated the release of ROS in BAL cells in response to CS exposure (Figure 7C). Furthermore, genetic knockout of p21 decreased the levels of lung lipid peroxidation products (4-HNE and MDA) in response to CS exposure (Figure 7B). These results suggested that CS-induced ROS release and lipid peroxidation were dependent, at least in part, on p21 level in the lungs, and genetic knockout of p21 reduced the oxidative burden particularly caused by CS.

Phosphorylated and Total Levels of NF-κB RelA/p65 Were Decreased in Lungs of p21−/− Mice in Response to CS Exposure

NF-κB activation plays an important role in CS-mediated lung inflammation (5, 6, 8, 10, 53). In light of our data showing reduced lung inflammatory in lungs of p21−/− mice exposed to CS, we determined the nuclear levels of RelA/p65 and its phosphorylation on ser276 and ser536 residues in lungs of WT and p21−/− mice with or without CS exposure. Western blot analysis showed that CS exposure led to an increase in RelA/p65 and its phosphorylation at ser276 and ser536 residues in lung nuclear fraction in WT mice (Figures 8A and 8B). Targeted disruption of p21 decreased the levels of both phosphorylated and total RelA/p65 (ser276 and ser526) in the lungs in response to CS exposure (Figures 8A and 8B). These results suggested that decreased phosphorylation of RelA/p65 might contribute to reduced level of RelA/p65 leading to decreased release of NF-κB–dependent pro-inflammatory mediators in lungs of p21−/− mice exposed to CS.

IKKβ Activity Was Decreased in Lungs of p21−/− Mice in Response to CS Exposure

It has been shown that IKKβ is directly involved in phosphorylation and degradation of inhibitory IκBα, leading to subsequent NF-κB activation in response to a variety of inflammatory stimuli. Moreover, RelA/p65 can also be phosphorylated by IKKβ at the residues of ser536 and ser468 (54, 55). Based on the reduced activation of NF-κB in lungs of p21−/− mice exposed to CS, we determined the IKKβ activity in lungs of both WT and p21−/− mice. As shown in Figures 9A and 9B, the IKKβ activity was decreased in lungs of p21−/− mice compared with WT mice exposed to CS, suggesting that genetic ablation of p21 resulted in reduction of IKKβ–NF-κB signals in response to CS exposure.

Decreased Release of MCP-1 and KC in Peritoneal Macrophages from p21−/− Mice

To further investigate whether decreased NF-κB activation is one of the mechanisms underlying decreased inflammatory response in lungs of these KO mice in response to CS exposure, peritoneal macrophages from WT and p21-deficient mice were isolated and treated with CSE. Consistent with the *in vivo* results, NF-κB–dependent pro-inflammatory mediators such as MCP-1 and KC were significantly increased in response to CSE (0.1%, 0.2%, and 0.4%) in peritoneal macrophages derived from WT mice. However, this response was significantly decreased in peritoneal macrophages obtained from p21−/− mice compared with WT mice in response to CSE treatment (Figure 10). These data suggest that reduced inflammatory response was associated with decreased NF-κB activation in p21−/− mice in response to CS exposure.

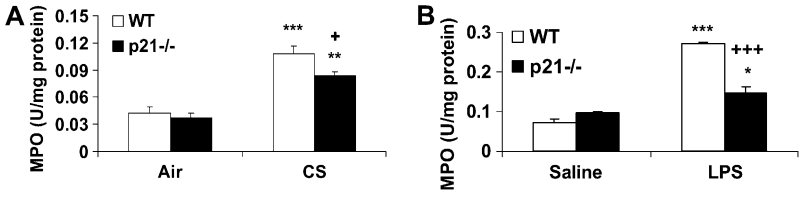

Figure 4. Myeloperoxidase (MPO) activity was decreased in lungs of p21−/− mice exposed to CS or aerosolized to LPS. Lung sections from mice exposed to CS (*A*) or aerosolized to LPS (*B*) were homogenized, and the MPO activity was determined spectrophotometrically. Targeted ablation of p21 decreased the MPO activity in the lungs in response to CS and LPS exposure. Data are shown as mean ± SEM (n = 3–4 per group). *$P < 0.05$, **$P < 0.01$, ***$P < 0.001$, significant compared with respective air- or saline-exposed group; $^{+}P < 0.05$, $^{+++}P < 0.001$, significant compared with CS- or LPS-exposed WT mice.

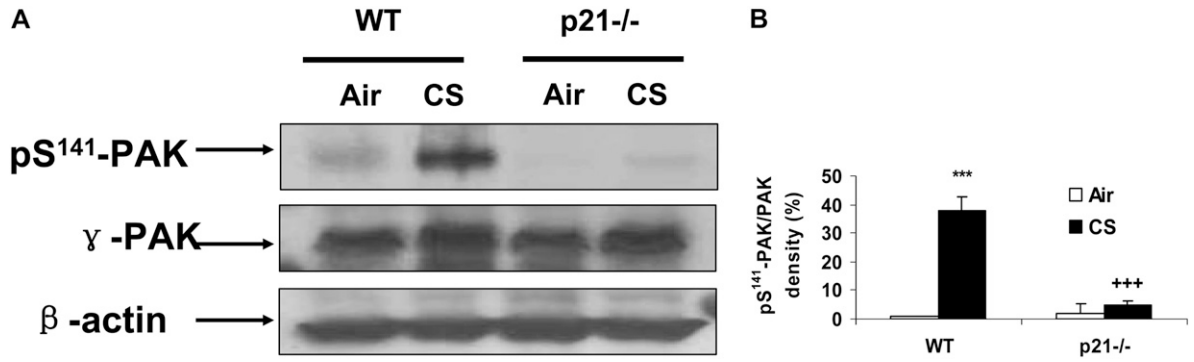

Figure 5. Phosphorylated level of p21-activated kinase (PAK) was decreased in lung cytosolic protein of p21−/− mice in response to CS exposure. The protein levels of γ-PAK and its phosphorylation on ser141 residue from air- and CS-exposed mice were analyzed by Western blotting as described in MATERIALS AND METHODS, and β-actin was used as an indicator for equal protein loading. (*A*) Representative blotting bands. (*B*) Graphic summary of densitometric analysis of Western blotting bands from three independent experiments (n = 3–4 per group). The level of phosphorylated PAK was decreased in lung cytosolic protein of p21−/− mice exposed to CS. ***$P < 0.001$, significant compared with respective air-exposed group; $^{+++}P < 0.001$, significant compared with CS-exposed WT mice.

DISCUSSION

Cigarette smoke is a strong pro-inflammatory stimulus that induces the release of pro-inflammatory mediators by recruiting macrophages and neutrophils into the lung tissue (6, 11, 37, 38, 45, 56). We, and others, have shown that p21 expression was increased in alveolar macrophages from smokers (28) and in lung epithelial cells and fibroblasts in response to CS (29–31). In addition, oxidant-induced DNA damage prolonged the expression of p21 (32). Most importantly, p21 is also involved in

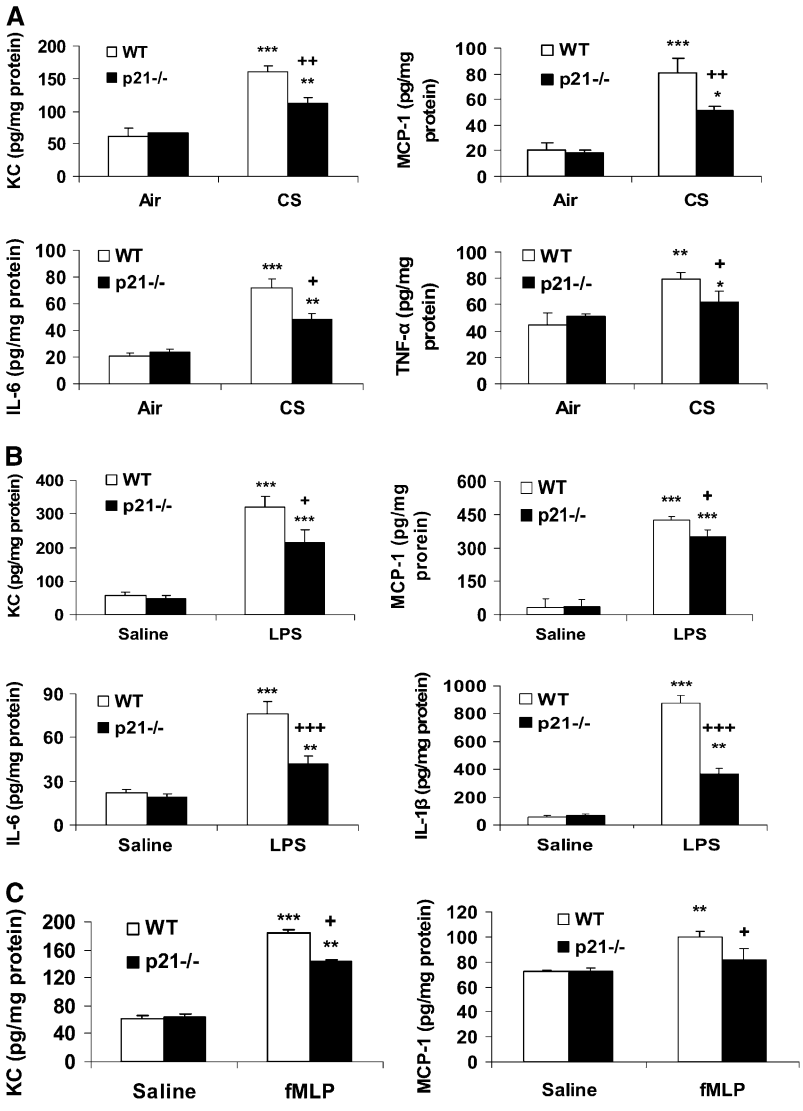

Figure 6. Levels of pro-inflammatory mediators were decreased in lungs of p21−/− mice in response to CS exposure, LPS, and fMLP aerosolization. Mice were exposed to CS, LPS, and fMLP as described in MATERIALS AND METHODS. Pro-inflammatory mediators in the lungs were measured by luminex assay in response to (*A*) CS exposure, (*B*) LPS, and (*C*) fMLP aerosolization. The levels of pro-inflammatory mediators in the lungs were increased in WT mice, but were decreased in p21−/− mice as compared to WT mice exposed to CS, LPS, and fMLP. Data are shown as mean ± SEM (n = 3–4 per group). *$P < 0.05$, **$P < 0.01$, ***$P < 0.001$, significant compared with respective air- or saline-exposed group; $^{+}P < 0.05$, $^{++}P < 0.01$, $^{+++}P < 0.001$, significant compared with CS-, LPS-, or fMLP-exposed WT mice.

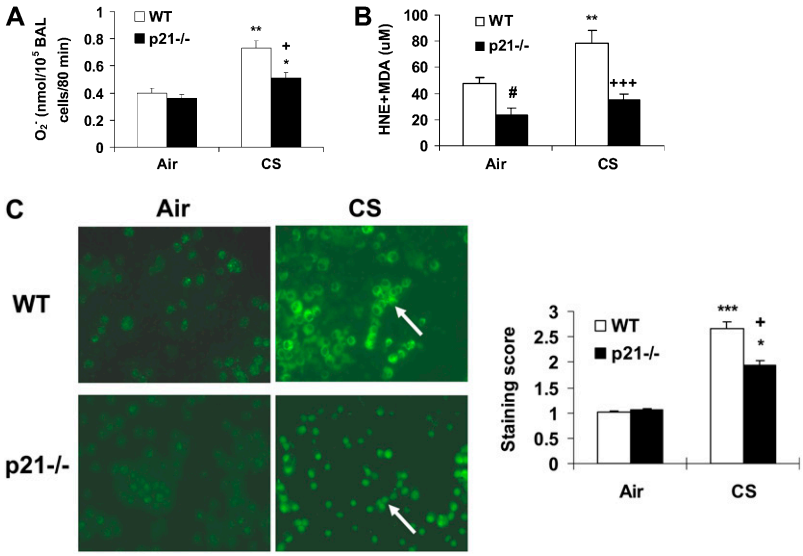

Figure 7. Levels of oxidative stress markers (reactive oxygen species [ROS] release in BAL cells and lipid peroxidation products in lungs) were reduced in p21−/− mice in response to CS exposure. (*A*) BAL cells from air- or CS-exposed mice were incubated with or without PMA. Release of superoxide anion was determined by the reduction of ferricytochrome *c* after 80 minutes of stimulation as described in MATERIALS AND METHODS. (*B*) Mice were exposed to CS and levels of 4-HNE plus MDA were measured spectrophotometrically in the lungs as described in MATERIALS AND METHODS. Data are shown as mean ± SEM (n = 3–4 per group). (*C*) BAL cells on the cytospin slides from CS-exposed mice were incubated with DCF-DA. After being rinsed with PBS, the slides were observed under fluorescent microscope. The figures are representative of three independent staining experiments (n = 3–4 per group). *Arrows* indicate ROS in BAL cells. *Original magnification*: ×400. Genetic ablation of p21 attenuated ROS release in BAL cells and lipid peroxidation products in lungs in response to CS exposure. $^{*}P < 0.05$, $^{**}P < 0.01$, $^{***}P < 0.001$, significant compared with respective air-exposed mice; $^{+}P < 0.05$, $^{+++}P < 0.001$, significant compared with CS-exposed WT mice; $^{\#}P < 0.05$, compared with air-exposed WT mice.

inflammatory response in the model of atherosclerosis (24) in addition to its regulatory effect on cell cycle. Recent evidence suggested that cellular senescence and proliferation/apoptosis, which are regulated by p21, are involved in pathophysiology of emphysema/COPD (12). However, the role of p21 in CS-induced lung inflammatory and injurious responses is not known. We hypothesized that targeted ablation of p21 protects the lungs against detrimental effect of CS. Consistent with its pro-inflammatory effect of p21 seen *in vivo* and *in vitro* (24, 25, 27), genetic knockout of p21 attenuated the lung inflammatory response, such as inflammatory cell influx, release of pro-inflammatory mediators, and MPO activity, in the lungs of mice exposed to CS. Recent studies showed that phosphorylation of PAK is the key step in activation of PAK leading to neutrophil influx into the lungs in response to LPS inhalation (51). Our data show that genetic ablation of p21 decreased phosphorylation of PAK by CS exposure, implying that this may be the mechanism for reduced pro-inflammatory effects of CS in the lungs of these mice. In addition, to confirm the role of p21 in pro-inflammatory response, we used the bacterial endotoxin and fMLP to induce lung inflammation and injury, particularly fMLP to induce airspace enlargement (emphysema) in mice (5,

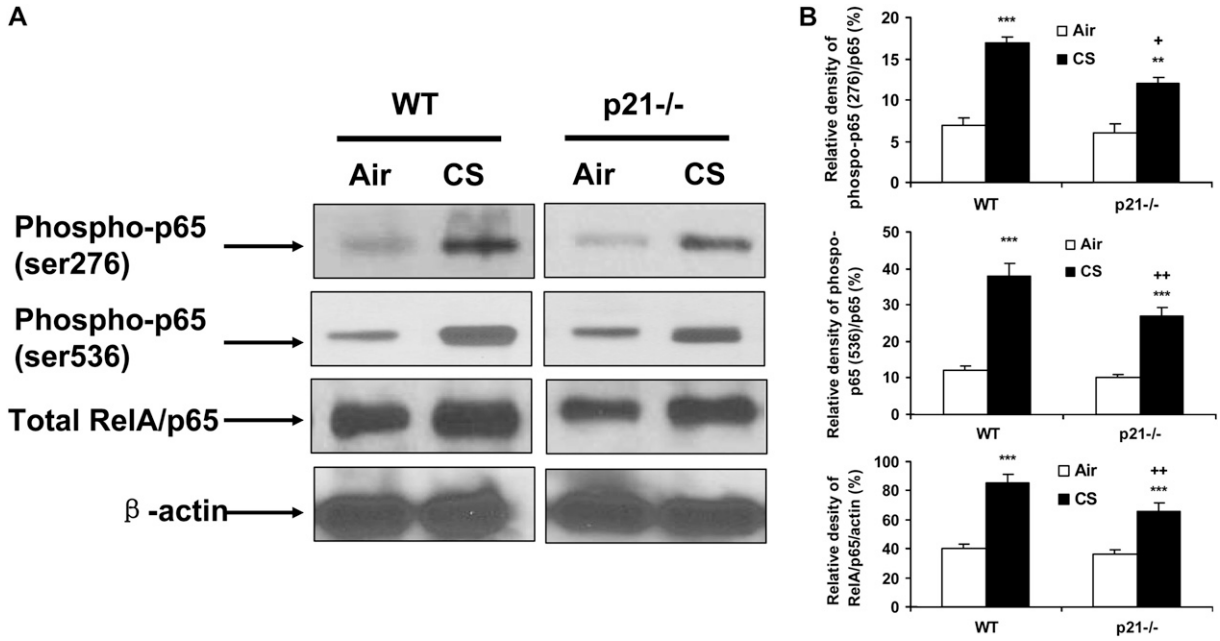

Figure 8. Phosphorylated and total levels of RelA/p65 were decreased in lung nuclear protein of p21−/− mice in response to CS exposure. The levels of RelA/p65 and its phosphorylation on ser276 and ser536 residues in the lungs from air- and CS-exposed mice were analyzed by Western blotting as described in MATERIALS AND METHODS, and β-actin was used as an indicator for equal protein loading. (*A*) Representative blotting bands. (*B*) Graphic summary of densitometric analysis of Western blotting bands from three independent experiments (n = 3–4 per group). The levels of phosphorylated and total RelA/p65 were reduced in the lungs of p21−/− mice compared with WT mice in response to CS. $^{**}P < 0.01$, $^{***}P < 0.001$, significant compared with respective air-exposed mice; $^{+}P < 0.05$, $^{++}P < 0.01$, significant compared with CS-exposed WT mice.

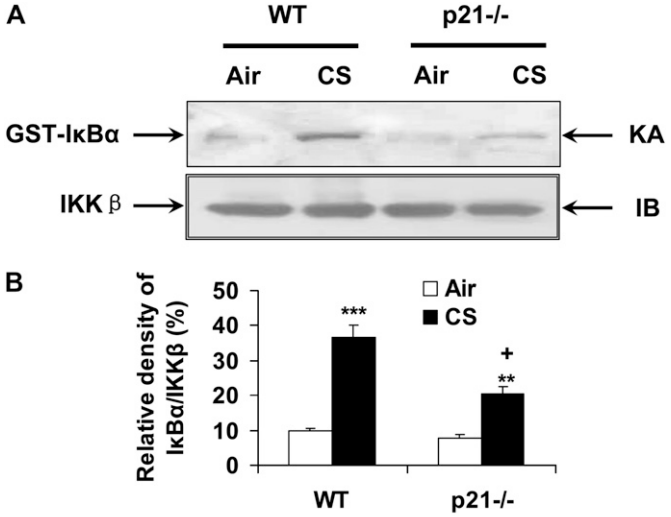

Figure 9. IKKβ activity was attenuated in lungs of p21−/− mice in response to CS exposure. Whole cell extracts from mouse lung tissue were immunoprecipitated with an antibody against IKKβ, and the immunoprecipitates were subjected to kinase assay (KA) using GST-IκBα as substrate. The samples were subjected to SDS-PAGE and transferred onto PVDF membranes and were exposed to a film. Equal amount of the immunoprecipitated kinase complex were confirmed by immunoblotting (IB) for IKKβ. (*A*) Representative blotting bands. (*B*) Graphic summary of densitometric analysis of blotting bands from three independent experiments (n = 3–4 per group). The IKKβ activity was attenuated in lungs of p21−/− mice in response to CS. $^{**}P < 0.01$, $^{***}P < 0.001$, significant compared with respective air-exposed group; $^{+}P < 0.05$, significant compared with CS-exposed WT mice.

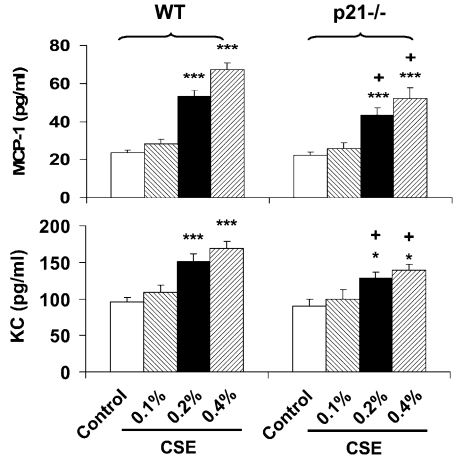

Figure 10. Decreased levels of monocyte chemotactic protein (MCP)-1 and keratinocyte chemoattractant (KC) in peritoneal macrophages from p21−/− mice in response to CSE treatment. Peritoneal macrophages were isolated from WT and p21−/− mice, and treated with CSE (0.1, 0.2, and 0.4%). CSE induced the release of MCP-1 and KC from peritoneal macrophages of WT mice; this release was attenuated in peritoneal macrophages from p21−/− mice. Data are shown as mean ± SEM (n = 4–5 per group). $^{*}P < 0.05$, $^{***}P < 0.001$, significant compared with respective control group; $^{+}P < 0.05$, significant compared with respective CSE-treated peritoneal macrophages from WT mice.

33–35, 47). It was interesting to observe that inflammatory cell influx into the lungs was significantly reduced in lungs of p21-deficient mice as compared with WT mice in response to aerosolized LPS or fMLP. Furthermore, the MPO activity in lungs was also decreased in p21−/− mice in response to LPS aerosolization. Mostly importantly, to show protection against airspace enlargement, we used the fMLP-induced airspace enlargement, which mimics chronic CS-induced emphysema (33, 34). It is interesting to note that genetic knockout of p21 decreased fMLP-mediated airspace enlargement. These results suggested that knockout of p21 gene leads to protection against pro-inflammatory and injurious effects of CS, LPS, and fMLP in lungs of these mice.

Our preliminary data showed that the levels of chemokines in BAL fluid were lower than these in lung homogenate, although the levels of chemokines were increased in both BAL fluid and lung homogenate of WT and p21−/− in response to CS exposure (H. Yao and coworkers, unpublished observations). It is possible that the chemokines gradient between BAL fluid and lung tissue will attract more macrophages into the lungs (interstitium), which may be one of the reasons why there was no change in number of macrophages in the BAL fluid whereas the number of macrophages in lung interstitium was increased in both WT and p21−/− mice in response to CS exposure. Therefore, a significantly decreased level of chemokines in lung homogenate of p21−/− mice may contribute to the decreased number of macrophages in lung interstitium of p21−/− mice compared with WT mice in response to acute CS exposure.

Although the number of neutrophils in BAL fluid in fMLP groups was very low compared with LPS- and CS-exposed groups in WT and p21−/− mice, we could not exclude the possibility that fMLP induced a continuous recruitment of neutrophils into the lung interstitium that is not reflected by the number of neutrophils in BAL fluid. Indeed, elastase derived from neutrophils is long-lived in lung septa, which contributes to alveolar destruction induced by fMLP (33, 34). Furthermore, the level of KC, a potent neutrophil chemokine, in lung homogenate of fMLP-exposed mice was comparable to that of CS- or LPS-exposed mice. These data suggested that neutrophils are continuously recruited into the lung interstitium in response to fMLP. This may be the reason for our observation that the level of KC was comparable whereas the number of neutrophils in BAL fluid is low compared with LPS- and CS-exposed groups in response to fMLP aerosolization.

CS induces endogenous production of ROS such as superoxide anions, hydrogen peroxide, and hydroxyl radicals. We have shown that leukocytes isolated from smokers and from patients with COPD release elevated levels of superoxide anions (56, 57), which was associated with increased systemic levels of inflammatory mediators (9, 58). Consistent with the previous study (39), CS exposure resulted in an increase in ROS release and lipid peroxidation products, as shown by release of superoxide anion and DCF-DA staining in BAL cells, and 4-HNE and MDA contents in lung homogenates of WT mice. Targeted disruption of p21 decreased the release of ROS and products of lipid peroxidation in the lungs in response to CS exposure. Phosphorylation of $p47^{phox}$ is a key step in the translocation of the cytoplasmic components of NADPH oxidase into the cell membrane, where they form the active NADPH oxidase, thus generating cellular ROS (59). Recent studies show that PAK activity is required for efficient ROS generation in human neutrophils by phosphorylating $p47^{phox}$ on serine residues at ser141 and thr423 (60, 61). We observed that CS exposure led to an increased phosphorylation of PAK (ser141) and $p47^{phox}$ (serine residues) in WT mice, which was decreased in p21−/− mice (data not shown). Therefore, the reduced ROS release seen in genetically ablated p21 mice in

response to CS exposure may be associated with the decreased phosphorylation of $p47^{phox}$ by inactivating PAK compared with WT mice in response to CS exposure. Recently, it has been shown that inhibition of p21-mediated ROS accumulation can rescue p21-induced senescence (21). Therefore, reduced levels of ROS in p21−/− mice may rescue CS-induced senescence of lung cells, and explain the attenuation of lung inflammatory response induced by CS and other pro-inflammatory agents.

In quiescent cells, NF-κB activity is mainly controlled by its tight association with the IκB protein, which prevents NF-κB from entering into the nucleus (53, 62). It has been shown that IKKβ activates NF-κB by regulating the phosphorylation, ubiquitination, and degradation of IκB in response to diverse stimuli. Furthermore, RelA/p65 can also be phosphorylated by IKKβ at the residues of ser536 and ser468 (54, 55). Our data show that the IKKβ activity and total nuclear level of RelA/p65 were decreased in lungs of p21−/− mice compared with WT mice in response to CS exposure. Furthermore, the release of NF-κB–dependent pro-inflammatory mediators, such as KC and MCP-1, was also reduced from peritoneal macrophages of p21−/− mice compared with WT mice in response to CSE treatment. Therefore, these data demonstrated the reduced activation of NF-κB in lungs of p21−/− mice in response to CS exposure. Post-translational modification of NF-κB members is believed to represent a second level of regulating NF-κB activity (62–64). Several different phosphorylation sites have been mapped for activating NF-κB RelA/p65 subunit (62, 64). In our study, we observed an increased level of phosphorylation in RelA/p65 on ser276 and ser536 residues in lung nuclear proteins of WT mice in response to CS exposure, and this phosphorylation pattern was reduced in p21−/− mice. Previous studies demonstrated that phosphorylation of RelA/p65 on ser276 residue is required for association with CBP and NF-κB transcriptional activity (65, 66). Therefore, our data showing reduced phosphorylation of RelA/p65 expression will lead to decreased interaction of RelA/p65 with co-activator CBP in p21−/− mice. This observation is corroborated by studies showing that p21 stimulate NF-κB activity through its effect on the CBP/p300 transcription cofactor family, and genetic ablation was associated with attenuation of NF-κB activation in response to LPS in glial cells (27). Furthermore, it is known that phosphorylation of ser536 on RelA/p65 is a prerequisite for acetylation of lysine 310 on RelA/p65, which is required for full and sustained transactivation by NF-κB–transactivator complex leading to sustained pro-inflammatory gene expression (6, 67). Recently, we have shown that acetylation of RelA/p65 plays an important role in sustained inflammatory gene transcription in the lungs of rats exposed to CS (6). Thus, reduced phosphorylation of RelA/p65 on ser536 might contribute to decreased acetylation of RelA/p65 and subsequent decreased inflammatory response in p21−/− mice exposed to CS. However, further studies are required to determine the mechanism of RelA/p65 regulation and chromatin remodeling by CBP in p21−/− mice exposed to CS.

Previous studies showed that ROS is not necessarily directly related to NF-κB activation (68, 69). However, a direct or indirect link between ROS release and NF-κB activation is not clear in the present system, although both of these parameters were decreased in lungs of p21−/− mice compared with WT mice in response to CS exposure. Nevertheless, based on our *in vivo* and *in vitro* data, the reduced lung inflammatory response was associated with decreased NF-κB activation in peritoneal macrophages and ROS release from BAL cells obtained from p21−/− mice in response to CS.

Cellular senescence is a state of irreversible growth arrest induced either by telomere shortening or by telomere-independent signals, such as DNA damage and oxidative stress. CS-derived ROS are known to induce cellular senescence in alveolar epithelial cells and lung fibroblasts *in vitro* and *in vivo* (29, 30), which contribute to impaired re-epithelialization. Recently, a new concept was proposed on cellular senescence/proliferation and apoptosis in the pathogenesis of COPD (emphysema) (12–14, 70). It is well known that p21 is an important protein involved in cellular senescence (29, 30). Our preliminary data showed that the reduced cell senescence and redressing the imbalance of apoptosis/proliferation in lung cells might confer the protection against detrimental effects of CS in lungs of p21 ablated mice (H. Yao and colleagues, unpublished observations). In the present study, the data showing protection of oxidative, inflammatory, and injurious responses in p21−/− mice (defective in G1 checkpoint control) suggests a key role of p21 in underlying abnormal inflammation in susceptible smokers. Further studies are in progress to understand the mechanism of protection of p21−/− against CS-induced airspace enlargement, oxidative (ROS generation) and pro-inflammatory responses (NF-κB-CBP chromatin remodeling on pro-inflammatory gene promoters), and identification of cell types involved in senescence, proliferation, and apoptosis in lungs of p21−/− mice in response to chronic CS exposure.

In summary, our data show that targeted disruption of p21 attenuates CS-, LPS-, or fMLP-mediated lung inflammatory responses. CS-mediated oxidative stress, and fMLP-induced airspace enlargement, are also decreased in lungs of p21−/− mice compared with WT mice. These findings are associated with decreased NF-κB activation and ROS release. The possible molecular mechanism of down-regulation of ROS release is due to decreased phosphorylation of $p47^{phox}$ by down-modulating the activation of PAK in p21−/− mice in response to CS exposure. Reduction in inflammatory responses and oxidative stress in p21−/− mice in response to CS exposure may have an effect on redressing the imbalance of cell senescence/proliferation and hence conferring protection against airspace enlargement. Overall, our data may have ramifications in CS-induced senescence/apoptosis in the pathogenesis of COPD/emphysema.

Conflict of Interest Statement: None of the authors has a financial relationship with a commercial entity that has an interest in the subject of this manuscript.

Acknowledgments: The authors thank Dr. Aruna Kode for providing technical assistance. They also thank Dr. T. Rangasamy for useful discussions during the preparation of this manuscript.

References

1. Hogg JC, Chu F, Utokaparch S, Woods R, Elliott WM, Buzatu L, Cherniack RM, Rogers RM, Sciurba FC, Coxson HO, *et al.* The nature of small-airway obstruction in chronic obstructive pulmonary disease. *N Engl J Med* 2004;350:2645–2653.
2. Gan WQ, Man SF, Senthilselvan A, Sin DD. Association between chronic obstructive pulmonary disease and systemic inflammation: a systematic review and a meta-analysis. *Thorax* 2004;59:574–580.
3. Jeffery PK. Remodeling and inflammation of bronchi in asthma and chronic obstructive pulmonary disease. *Proc Am Thorac Soc* 2004;1: 176–183.
4. Church DF, Pryor WA. Free-radical chemistry of cigarette smoke and its toxicological implications. *Environ Health Perspect* 1985;64:111–126.
5. Thatcher TH, Maggirwar SB, Baglole CJ, Lakatos HF, Gasiewicz TA, Phipps RP, Sime PJ. Aryl hydrocarbon receptor-deficient mice develop heightened inflammatory responses to cigarette smoke and endotoxin associated with rapid loss of the nuclear factor-kappaB component RelB. *Am J Pathol* 2007;170:855–864.
6. Yang SR, Wright J, Bauter M, Seweryniak K, Kode A, Rahman I. Sirtuin regulates cigarette smoke-induced pro-inflammatory mediator release via RelA/p65 NF-kappaB in macrophages in vitro and in rat lungs in vivo: implications for chronic inflammation and aging. *Am J Physiol Lung Cell Mol Physiol* 2007;292:L567–L576.

7. Kode A, Yang SR, Rahman I. Differential effects of cigarette smoke on oxidative stress and proinflammatory cytokine release in primary human airway epithelial cells and in a variety of transformed alveolar epithelial cells. *Respir Res* 2006;7:132–151.
8. Yang SR, Chida AS, Bauter MR, Shafiq N, Seweryniak K, Maggirwar SB, Kilty I, Rahman I. Cigarette smoke induces proinflammatory cytokine release by activation of NF-kappaB and posttranslational modifications of histone deacetylase in macrophages. *Am J Physiol Lung Cell Mol Physiol* 2006;291:L46–L57.
9. Rahman I, Adcock IM. Oxidative stress and redox regulation of lung inflammation in COPD. *Eur Respir J* 2006;28:219–242.
10. Moodie FM, Marwick JA, Anderson CS, Szulakowski P, Biswas SK, Bauter MR, Kilty I, Rahman I. Oxidative stress and cigarette smoke alter chromatin remodeling but differentially regulate NF-kappaB activation and proinflammatory cytokine release in alveolar epithelial cells. *FASEB J* 2004;18:1897–1899.
11. Bracke KR, D'Hulst AI, Maes T, Moerloose KB, Demedts IK, Lebecque S, Joos GF, Brusselle GG. Cigarette smoke-induced pulmonary inflammation and emphysema are attenuated in CCR6-deficient mice. *J Immunol* 2006;177:4350–4359.
12. Yoshida T, Tuder RM. Pathobiology of cigarette smoke-induced chronic obstructive pulmonary disease. *Physiol Rev* 2007;87:1047–1082.
13. Tsuji T, Aoshiba K, Nagai A. Alveolar cell senescence in patients with pulmonary emphysema. *Am J Respir Crit Care Med* 2006;174:886–893.
14. Calabrese F, Giacometti C, Beghe B, Rea F, Loy M, Zuin R, Marulli G, Baraldo S, Saetta M, Valente M. Marked alveolar apoptosis/proliferation imbalance in end-stage emphysema. *Respir Res* 2005;6:14–26.
15. Heichman KA, Roberts JM. Rules to replicate by. *Cell* 1994;79:557–562.
16. O'Reilly MA. DNA damage and cell cycle checkpoints in hyperoxic lung injury: braking to facilitate repair. *Am J Physiol Lung Cell Mol Physiol* 2001;281:L291–L305.
17. Ekholm SV, Reed SI. Regulation of G(1) cyclin-dependent kinases in the mammalian cell cycle. *Curr Opin Cell Biol* 2000;12:676–684.
18. Sherr CJ, Roberts JM. CDK inhibitors: positive and negative regulators of G1-phase progression. *Genes Dev* 1999;13:1501–1512.
19. Sherr CJ, Roberts JM. Inhibitors of mammalian G1 cyclin-dependent kinases. *Genes Dev* 1995;9:1149–1163.
20. Harper JW, Elledge SJ, Keyomarsi K, Dynlacht B, Tsai LH, Zhang P, Dobrowolski S, Bai C, Connell-Crowley L, Swindell E, *et al.* Inhibition of cyclin-dependent kinases by p21. *Mol Biol Cell* 1995;6:387–400.
21. Macip S, Igarashi M, Fang L, Chen A, Pan ZQ, Lee SW, Aaronson SA. Inhibition of p21-mediated ROS accumulation can rescue p21-induced senescence. *EMBO J* 2002;21:2180–2188.
22. Marcotte R, Wang E. Replicative senescence revisited. *J Gerontol A Biol Sci Med Sci* 2002;57:B257–B269.
23. Scatizzi JC, Hutcheson J, Bickel E, Woods JM, Klosowska K, Moore TL, Haines GK III, Perlman H. p21Cip1 is required for the development of monocytes and their response to serum transfer-induced arthritis. *Am J Pathol* 2006;168:1531–1541.
24. Merched AJ, Chan L. Absence of p21Waf1/Cip1/Sdi1 modulates macrophage differentiation and inflammatory response and protects against atherosclerosis. *Circulation* 2004;110:3830–3841.
25. Kunieda T, Minamino T, Nishi J, Tateno K, Oyama T, Katsuno T, Miyauchi H, Orimo M, Okada S, Takamura M, *et al.* Angiotensin II induces premature senescence of vascular smooth muscle cells and accelerates the development of atherosclerosis via a p21-dependent pathway. *Circulation* 2006;114:953–960.
26. Perkins ND, Felzien LK, Betts JC, Leung K, Beach DH, Nabel GJ. Regulation of NF-kappaB by cyclin-dependent kinases associated with the p300 coactivator. *Science* 1997;275:523–527.
27. Tusell JM, Saura J, Serratosa J. Absence of the cell cycle inhibitor p21Cip1 reduces LPS-induced NO release and activation of the transcription factor NF-kappaB in mixed glial cultures. *Glia* 2005;49:52–58.
28. Tomita K, Caramori G, Lim S, Ito K, Hanazawa T, Oates T, Chiselita I, Jazrawi E, Chung KF, Barnes PJ, *et al.* Increased p21(CIP1/WAF1) and B cell lymphoma leukemia-x(L) expression and reduced apoptosis in alveolar macrophages from smokers. *Am J Respir Crit Care Med* 2002;166:724–731.
29. Nyunoya T, Monick MM, Klingelhutz A, Yarovinsky TO, Cagley JR, Hunninghake GW. Cigarette smoke induces cellular senescence. *Am J Respir Cell Mol Biol* 2006;35:681–688.
30. Tsuji T, Aoshiba K, Nagai A. Cigarette smoke induces senescence in alveolar epithelial cells. *Am J Respir Cell Mol Biol* 2004;31:643–649.
31. Marwick JA, Kirkham P, Gilmour PS, Donaldson K, Mac NW, Rahman I. Cigarette smoke-induced oxidative stress and TGF-beta1 increase p21waf1/cip1 expression in alveolar epithelial cells. *Ann N Y Acad Sci* 2002;973:278–283.
32. Chen QM, Bartholomew JC, Campisi J, Acosta M, Reagan JD, Ames BN. Molecular analysis of H2O2-induced senescent-like growth arrest in normal human fibroblasts: p53 and Rb control G1 arrest but not cell replication. *Biochem J* 1998;332:43–50.
33. Cavarra E, Martorana PA, de Santi M, Bartalesi B, Cortese S, Gambelli F, Lungarella G. Neutrophil influx into the lungs of beige mice is followed by elastolytic damage and emphysema. *Am J Respir Cell Mol Biol* 1999;20:264–269.
34. Cavarra E, Martorana PA, Gambelli F, de Santi M, van Even P, Lungarella G. Neutrophil recruitment into the lungs is associated with increased lung elastase burden, decreased lung elastin, and emphysema in alpha 1 proteinase inhibitor-deficient mice. *Lab Invest* 1996;75:273–280.
35. Peters MJ, Panaretto K, Breslin AB, Berend N. Effects of prolonged inhalation of N-formyl-methionyl-leucyl-phenylalanine in rabbits. *J Appl Physiol* 1991;70:2448–2454.
36. Deng C, Zhang P, Harper JW, Elledge SJ, Leder P. Mice lacking p21CIP1/WAF1 undergo normal development, but are defective in G1 checkpoint control. *Cell* 1995;82:675–684.
37. Thatcher TH, McHugh NA, Egan RW, Chapman RW, Hey JA, Turner CK, Redonnet MR, Seweryniak KE, Sime PJ, Phipps RP. Role of CXCR2 in cigarette smoke-induced lung inflammation. *Am J Physiol Lung Cell Mol Physiol* 2005;289:L322–L328.
38. Marwick JA, Kirkham PA, Stevenson CS, Danahay H, Giddings J, Butler K, Donaldson K, Macnee W, Rahman I. Cigarette smoke alters chromatin remodeling and induces proinflammatory genes in rat lungs. *Am J Respir Cell Mol Biol* 2004;31:633–642.
39. Foronjy RF, Mirochnitchenko O, Propokenko O, Lemaitre V, Jia Y, Inouye M, Okada Y, D'Armiento JM. Superoxide dismutase expression attenuates cigarette smoke- or elastase-generated emphysema in mice. *Am J Respir Crit Care Med* 2006;173:623–631.
40. Nadziejko C, Fang K, Bravo A, Gordon T. Susceptibility to pulmonary hypertension in inbred strains of mice exposed to cigarette smoke. *J Appl Physiol* 2007;102:1780–1785.
41. Hautamaki RD, Kobayashi DK, Senior RM, Shapiro SD. Requirement for macrophage elastase for cigarette smoke-induced emphysema in mice. *Science* 1997;277:2002–2004.
42. Marwick JA, Stevenson CS, Giddings J, MacNee W, Butler K, Rahman I, Kirkham PA. Cigarette smoke disrupts VEGF165-VEGFR-2 receptor signaling complex in rat lungs and patients with COPD: morphological impact of VEGFR-2 inhibition. *Am J Physiol Lung Cell Mol Physiol* 2006;290:L897–L908.
43. Kawakami M, Paul JL, Thurlbeck WM. The effect of age on lung structure in male BALB/cNNia inbred mice. *Am J Anat* 1984;170:1–21.
44. Imai K, Mercer BA, Schulman LL, Sonett JR, D'Armiento JM. Correlation of lung surface area to apoptosis and proliferation in human emphysema. *Eur Respir J* 2005;25:250–258.
45. Foronjy RF, Mercer BA, Maxfield MW, Powell CA, D'Armiento J, Okada Y. Structural emphysema does not correlate with lung compliance: lessons from the mouse smoking model. *Exp Lung Res* 2005;31:547–562.
46. Rangasamy T, Cho CY, Thimmulappa RK, Zhen L, Srisuma SS, Kensler TW, Yamamoto M, Petrache I, Tuder RM, Biswal S. Genetic ablation of Nrf2 enhances susceptibility to cigarette smoke-induced emphysema in mice. *J Clin Invest* 2004;114:1248–1259.
47. Birrell MA, McCluskie K, Wong S, Donnelly LE, Barnes PJ, Belvisi MG. Resveratrol, an extract of red wine, inhibits lipopolysaccharide induced airway neutrophilia and inflammatory mediators through an NF-kappaB-independent mechanism. *FASEB J* 2005;19:840–841.
48. Johnston RB. Secretion of superoxide anion: methods for studying mononuclear phagocytes. New York: Academic Press; 1981. pp. 489–498.
49. LeBel CP, Ischiropoulos H, Bondy SC. Evaluation of the probe 2',7'-dichlorofluorescin as an indicator of reactive oxygen species formation and oxidative stress. *Chem Res Toxicol* 1992;5:227–231.
50. Carp H, Janoff A. Possible mechanisms of emphysema in smokers: *in vitro* suppression of serum elastase-inhibitory capacity by fresh cigarette smoke and its prevention by antioxidants. *Am Rev Respir Dis* 1978;118:617–621.
51. Reutershan J, Stockton R, Zarbock A, Sullivan GW, Chang D, Scott D, Schwartz MA, Ley K. Blocking p21-activated kinase reduces lipopolysaccharide-induced acute lung injury by preventing polymorphonuclear leukocyte infiltration. *Am J Respir Crit Care Med* 2007;175:1027–1035.

52. Rahman I. Oxidative stress, chromatin remodeling and gene transcription in inflammation and chronic lung diseases. *J Biochem Mol Biol* 2003;36:95–109.
53. Rahman I, MacNee W. Role of transcription factors in inflammatory lung diseases. *Thorax* 1998;53:601–612.
54. Sakurai H, Chiba H, Miyoshi H, Sugita T, Toriumi W. IkappaB kinases phosphorylate NF-kappaB p65 subunit on serine 536 in the transactivation domain. *J Biol Chem* 1999;274:30353–30356.
55. Schwabe RF, Sakurai H. IKKbeta phosphorylates p65 at S468 in transactivaton domain 2. *FASEB J* 2005;19:1758–1760.
56. Morrison D, Rahman I, Lannan S, MacNee W. Epithelial permeability, inflammation, and oxidant stress in the air spaces of smokers. *Am J Respir Crit Care Med* 1999;159:473–479.
57. Rahman I, Morrison D, Donaldson K, MacNee W. Systemic oxidative stress in asthma, COPD, and smokers. *Am J Respir Crit Care Med* 1996;154:1055–1060.
58. Rahman I. Oxidative stress in pathogenesis of chronic obstructive pulmonary disease: cellular and molecular mechanisms. *Cell Biochem Biophys* 2005;43:167–188.
59. Bedard K, Krause KH. The NOX family of ROS-generating NADPH oxidases: physiology and pathophysiology. *Physiol Rev* 2007;87:245–313.
60. Lei M, Lu W, Meng W, Parrini MC, Eck MJ, Mayer BJ, Harrison SC. Structure of PAK1 in an autoinhibited conformation reveals a multistage activation switch. *Cell* 2000;102:387–397.
61. Martyn KD, Kim MJ, Quinn MT, Dinauer MC, Knaus UG. p21-activated kinase (Pak) regulates NADPH oxidase activation in human neutrophils. *Blood* 2005;106:3962–3969.
62. Schmitz ML, Bacher S, Kracht M. I kappa B-independent control of NF-kappa B activity by modulatory phosphorylations. *Trends Biochem Sci* 2001;26:186–190.
63. Neumann M, Naumann M. Beyond IkappaBs: alternative regulation of NF-kappaB activity. *FASEB J* 2007;21:2642–2654.
64. Anrather J, Racchumi G, Iadecola C. cis-acting, element-specific transcriptional activity of differentially phosphorylated nuclear factor-kappa B. *J Biol Chem* 2005;280:244–252.
65. Okazaki T, Sakon S, Sasazuki T, Sakurai H, Doi T, Yagita H, Okumura K, Nakano H. Phosphorylation of serine 276 is essential for p65 NF-kappaB subunit-dependent cellular responses. *Biochem Biophys Res Commun* 2003;300:807–812.
66. Zhong H, May MJ, Jimi E, Ghosh S. The phosphorylation status of nuclear NF-kappa B determines its association with CBP/p300 or HDAC-1. *Mol Cell* 2002;9:625–636.
67. Chen LF, Williams SA, Mu Y, Nakano H, Duerr JM, Buckbinder L, Greene WC. NF-kappaB RelA phosphorylation regulates RelA acetylation. *Mol Cell Biol* 2005;25:7966–7975.
68. Rahman I, MacNee W. Regulation of redox glutathione levels and gene transcription in lung inflammation: therapeutic approaches. *Free Radic Biol Med* 2000;28:1405–1420.
69. Rahman I, Biswas SK, Jimenez LA, Torres M, Forman HJ. Glutathione, stress responses, and redox signaling in lung inflammation. *Antioxid Redox Signal* 2005;7:42–59.
70. Demedts IK, Demoor T, Bracke KR, Joos GF, Brusselle GG. Role of apoptosis in the pathogenesis of COPD and pulmonary emphysema. *Respir Res* 2006;7:53–62.